Lock-in and quasiperiodicity in hydrodynamically self-excited flames: experiments and modelling

Larry K.B. Li[a,*], Matthew P. Juniper[a]

[a]*Engineering Department, Cambridge University, Trumpington Street, Cambridge, CB2 1PZ, United Kingdom*

Abstract

In this experimental study, we apply acoustic forcing to a range of jet diffusion flames, motivated by the study of how thermoacoustic oscillations interact with hydrodynamic oscillations. These flames have regions of absolute instability at their base and this causes them to exhibit self-excited oscillations at discrete natural frequencies. We apply the forcing around these frequencies, at varying amplitudes, focusing on the response near lock-in. We then model the system as a forced van der Pol oscillator.

Our results show that, contrary to some expectations, a hydrodynamically self-excited flame oscillating at one frequency is sensitive to forcing at other frequencies. When forced at low amplitudes, the flame responds at both frequencies as well as several nearby frequencies, indicating quasiperiodicity. When forced at high amplitudes, however, it locks into the forcing. The critical forcing amplitude required for lock-in increases both with the strength of the instability and with the deviation of the forcing frequency from the natural frequency. Qualitatively, these features are accurately predicted by the forced van der Pol oscillator. There are, nevertheless, two features that are not predicted. First, when forced above its natural frequency, the flame is more susceptible to lock-in than when it is forced below its natural frequency. Second, once the flame locks in, its oscillations are weaker than those of the unforced flame. This last finding suggests that, for thermoacoustic systems, lock-in may not be as detrimental as it is thought to be.

Keywords: Absolute instability, global instability, combustion instability, thermoacoustic instability

1. Introduction

In the analysis of thermoacoustic systems, a flame is usually characterised by the way its heat release responds to acoustic forcing. This response depends on the hydrodynamic stability of the flame. Some flames, such as a premixed bunsen flame, are hydrodynamically globally stable. They respond only at the forcing frequency. Other flames, such as a jet diffusion flame, are hydrodynamically globally unstable. They oscillate at their own natural frequencies and are often assumed to be insensitive to low-amplitude forcing at other frequencies [1].

If a hydrodynamically globally unstable flame really is insensitive to forcing at other frequencies, then it should be possible to weaken thermoacoustic oscillations by de-tuning the frequency of the natural hydrodynamic mode from that of the natural acoustic modes. This would be very beneficial for industrial combustors.

1.1. Hydrodynamic global instability

Hydrodynamic global (or 'self-excited') oscillations can be found in both reacting and non-reacting flows. Examples include flickering of candle flames [2], bulging of jet diffusion flames [3], bulging of low-density jets [4], and vortex shedding in bluff-body wakes [5]. Such oscillations are termed 'hydrodynamic' because they arise from hydrodynamic mechanisms. In the above cases, for instance, they arise from inflexion points in the cross-stream profiles of axial velocity and become increasingly unstable as the density gradient steepens in the opposite direction to the velocity gradient [6].

In a jet diffusion flame, the heat release changes the density profile and hence the velocity profile through the action of buoyancy [7, 8]. Crucially, the inflexion point in the shear layer just outside the flame coincides with a steep density gradient in the opposite direction to the velocity gradient, making it absolutely unstable [7]. This causes a hydrodynamic global mode, which stretches the flame and modulates the heat release in synchronisation [9].

In this paper, we test and refute the assumption that hydrodynamically self-excited flames are insensitive to forcing. We do this by acoustically forcing a range of jet diffusion flames. We control the strength of their global instability by changing the coflow velocity and the fuel composition. For each flame, we examine the forced response over a range of frequencies (not just at the forcing frequency) and discover much richer be-

*Corresponding author
Email address: lkbl2@cam.ac.uk (Larry K.B. Li)

haviour than that which is reported in the literature. We then show that this behaviour is similar to that of a simple model: the forced van der Pol oscillator [10]. As well as providing new insight into the way acoustic oscillations interact with hydrodynamic oscillations, this paper provides a useful tool for describing and analysing such interactions.

2. Methodology

2.1. Experimental

The experiments are performed on a round coaxial injector[1] with jet diffusion flames created from mixtures of methane and nitrogen. The flames are forced sinusoidally by a loudspeaker mounted upstream, over a range of frequencies ($7 \leq f_f \leq 35$ Hz)[2] around the natural global frequency, f_n.

The forcing amplitude, A, is measured using the two-microphone method [11]. It is defined, at the injector plane, as the amplitude of the velocity perturbation at f_f normalised by the bulk jet velocity: $A \equiv |u'_{1,\,f_f}|/U_1$. At each f_f, A is incrementally increased to 0.90, even though lock-in often occurs earlier[3]. Lock-in is defined as being when f_n locks into f_f, leaving no sign of the natural global mode in the power spectral density (PSD). This is a qualitative change, which is easy to identify. The critical forcing amplitude at which lock-in occurs, A_{loc}, is found by inspecting the PSD.

The flame response is measured using a high-speed camera (Phantom V4.2) via broadband chemiluminescence at 180 frames s^{-1}. The intensity in each frame is summed across every pixel column, generating a time series (five pixel rows in height) at each axial station, $I(x/d_1)$. In this paper, however, only one axial station, $x/d_1 = 10$, is examined. This station is chosen for three reasons: (i) it is just far enough downstream that the chemiluminescent emission leads to a reliable signal-to-noise ratio without saturation; (ii) it is sufficiently far downstream that the global mode (if one exists) has time to grow and interact with the forcing; but (iii) it is not so far downstream that it coincides with the location of vortex roll up, where the strain rates can be high enough to cause local flame extinction, especially if high forcing amplitudes are used.

Two methods are used to control the strength of the hydrodynamic global instability. In the first, coflow air is added around the flame base. This reduces the shear and advects perturbations downstream, both of which weaken the instability. In the second, the relative concentrations of methane and nitrogen are changed. Reducing the methane concentration, for example, increases the stoichiometric mixture fraction. This causes the flame to shift towards the jet centreline, closer to the shear layer. The resultant changes to the density and velocity profiles are such that the flame becomes less unstable [12].

[1] Inner diameter, $d_1 = 6$ mm; outer diameter, $d_2 = 30$ mm.

[2] The f_f increment is 1 Hz, except if f_n is more than 0.25 Hz from an integer frequency value, in which case an additional setting, at the 0.5 Hz increment, is used.

[3] The A increment is usually 0.20, but is reduced to 0.050 around lock-in and to 0.025 if lock-in occurs at $A < 0.10$.

2.2. Modelling

The forced flame dynamics is modelled using the forced van der Pol (VDP) oscillator. As in the experiments, the forcing is sinusoidal (right hand term):

$$\ddot{x} - \epsilon(1 - x^2)\dot{x} + x = A_{vdp}\,\sin(\omega_f\, t), \tag{1}$$

where A_{vdp} is the forcing amplitude and ω_f is its angular frequency. The parameter ϵ, which controls the degree of self-excitation and nonlinear self-limitation, is fixed at an arbitrary small value of 0.1. The natural angular frequency, ω_n, is 1. Equation (1) is solved numerically using a fourth-order Runge–Kutta method. This is done for a range of forcing frequencies ($0.3 \leq \omega_f \leq 2.5$) and amplitudes ($0 \leq A_{vdp} \leq 0.4$) in order to replicate the experimental conditions.

3. Results

3.1. Experimental

Six different flames are studied (table 1): five globally unstable and one globally stable. For each flame, the total flow rate of the reactants is fixed at $5{\times}10^{-5}$ m^3 s^{-1}, giving a jet velocity of $U_1 = 1.77$ m s^{-1}.

The globally unstable flames (Flames 1–5) all have similar natural frequencies: $12.5 \leq f_n \leq 14.7$ Hz. Figure 1 shows an image sequence of Flame 5 oscillating through one unforced cycle. The globally stable flame (Flame 6) has two natural frequencies, 14.8 and 16.1 Hz, when unforced. These, however, are replaced by a lightly damped global mode, at $f_n = 14.3$ Hz, whenever forcing is applied, however small the amplitude and even if its frequency is far from f_n.

3.1.1. Before lock-in

First we examine the forced response before lock-in. We focus on Flame 5 because it exhibits most clearly the dynamics common to all five globally unstable flames. For f_f (at 16 Hz) slightly above f_n, Fig. 2a shows time traces of the intensity at five forcing amplitudes: $0.025 \leq A \leq 0.30$. For comparison, a time trace of the same signal from the same flame but without forcing is also shown (bottom). The corresponding PSD curves are shown in Fig. 2b.

When unforced, the flame has a global mode at a discrete natural frequency, represented in the PSD by a sharp peak at $f_n = 14.7$ Hz. There are similar, but weaker, peaks at the harmonics. The presence of harmonics indicates that the natural varicose oscillation of the flame is not perfectly sinusoidal.

When forced at a low amplitude ($A = 0.025$), the flame responds at f_f as well as f_n. Around these two frequencies, there are multiple spectral peaks. Known as sidebands, they are caused by nonlinear interactions

between the natural mode and the forcing. Their presence suggests that the flame is quasiperiodic, behaving like a typical forced oscillator before lock-in[4].

Additional spectral peaks arise at low frequencies, $f < 3$ Hz. Among these, the highest corresponds to the beat frequency: $|f_f - f_n|$. In the time traces (Fig. 2a), this beating phenomenon can be seen as low-frequency (long-wavelength) modulations of the signal amplitude.

As A increases from 0.025 to 0.050, f_n shifts towards f_f, which remains fixed. Once A reaches a critical value of 0.075, the natural mode locks into the forcing: the PSD becomes dominated by f_f and its harmonics (i.e. $2f_f$, $3f_f$,...), with no sign of the original natural mode. The PSD of the locked-in flame looks similar to that of the unforced flame, except that the dominant frequency is f_f. (Lock-in can also occur for $f_f < f_n$. For brevity, however, these results are not shown.)

The flame response at other forcing frequencies can be examined in the consolidated PSD: a contour plot of the PSD with the response frequency on the horizontal axis and f_f on the vertical axis. Fig. 3 shows this for Flame 5 forced at $A = 0.10$. The natural mode is indicated by a contiguous stripe that runs vertically at f_n through all values of f_f except those to which the flame is locked in. Its second ($2f_n$) and third ($3f_n$) harmonics are similarly indicated. At lock-in, the forcing dominates and the response therefore consists of a stripe along the diagonal for $f_f = f_n$. Although not shown, the f_f band in which lock-in occurs expands vertically as A increases (to be discussed in §3.1.2).

Away from lock-in, the nonlinear interactions between the natural mode and the forcing give rise to spectral peaks at low frequencies as well as around f_f and f_n (especially if the two are close). Further interactions occur between f_f and the harmonics of f_n, but not vice versa. The result is that between the vertical stripes marking f_n and its harmonics, there are spectral peaks set in a distinctive diamond pattern.

The above dynamics can be understood more easily by inspecting phase portraits and Poincaré maps. A phase portrait is a three-dimensional plot of the system motion (here the flame intensity) against that same motion shifted by a time delay, and by two time delays. A two-dimensional slice through that set of trajectories gives the Poincaré map. The Poincaré maps for Flame 5 forced at the conditions of Figs. 2a and 2b are shown in Fig. 2c. For clarity, these maps are cropped such that only half the (symmetrical) slice is shown.

For the unforced flame, the phase trajectory is closed, indicating that the flame oscillates periodically at a limit cycle (of f_n). A half-section of this trajectory contains data points scattered around one blob. If the system were free of noise, the trajectory would be perfectly closed and the cropped Poincaré map would show one discrete point.

As A increases, the phase trajectory follows the surface of a torus. In the cropped Poincaré map, this is seen as a ring. The appearance of a torus-like surface is characteristic of quasiperiodicity. For weak forcing ($A = 0.025$–0.050), the rings increase in size as A increases. For strong forcing ($A = 0.075$–0.30), they close again to another limit cycle, this time at f_f. The final limit cycle resembles the one for the unforced flame.

These results show that a self-excited flame responds to forcing in a manner more complicated than that which is expected from the literature. Before lock-in, the flame responds not only at its natural frequency, but also at the forcing frequency and at several other discrete frequencies. For combustion systems, this implies that thermoacoustic oscillations cannot be weakened simply by de-tuning the flame's natural frequency from the combustor's acoustic frequencies. In fact, the flame response at other frequencies may excite other acoustic modes.

3.1.2. Lock-in

Next we examine the forced response at lock-in. We start by considering the relationship between the minimum forcing amplitude required for lock-in, A_{loc}, and the normalised forcing frequency, f_f/f_n. This is shown in Fig. 4 for all six flames. The diagonal lines through the data around $f_f/f_n = 1$ are linear fits. For lock-in around the fundamental, the data at $f_f/f_n < 1$ are regressed separately from the data at $f_f/f_n > 1$. For lock-in around the subharmonic, the data are not regressed at all because the trends do not fit a linear model.

Several features are shared by all six flames. When f_f is close to f_n or $f_n/2$, A_{loc} is low. When f_f is far from f_n and $f_n/2$, A_{loc} is high. Around the fundamental, A_{loc} increases in proportion to $|f_f - f_n|$, indicating a Hopf bifurcation to a global mode. This linear relationship gives rise to $\vee$-shaped curves, similar to those found for other self-excited flows [4, 5, 13, 14]. For each flame, despite strong forcing ($A = 0.90$), there is a limit to how far f_f can deviate from f_n before lock-in is not possible: $f_f/f_n \approx 1.2$–1.4. Around the subharmonic, the relationship between A_{loc} and $|f_f - f_n|$ is not as linear as that around the fundamental, although the overall trends are similar.

Several differences exist between the six flames. As noted in §2.1, adding coflow weakens their global instability, which should make them more receptive to forcing, enabling lock-in to occur at lower A. Such behaviour is indeed observed when Flame 1 is compared to Flame 2, and when Flame 4 is compared to Flame 5. The flames with coflow (Flames 2 and 5) lock in more readily than do their counterparts without coflow (Flames 1 and 4). This is seen not only for f_f around f_n but also for f_f on the high-frequency side of $f_n/2$.

Another way to weaken global instability is to reduce the fuel concentration. According to Fig. 4, reducing $[CH_4]$ from 100% (Flame 1) to 80% (Flame 3) to 60% (Flame 4) has only a small effect on A_{loc}. Although the curves seem to shift downwards, the change is so small that it is within experimental uncertainty. Reducing $[CH_4]$ further to 40% (Flame 6), however, causes a marked decrease in the slopes of the $\vee$-shape. These findings suggest that the flame with a weak global mode

[4] In many dynamical systems, quasiperiodicity tends to arise when a self-excited oscillator is driven at a low amplitude and at a frequency that is not a rational multiple of the natural frequency.

(Flame 6) locks in more readily than do the flames with strong global modes (Flames 1, 3, and 4).

A final observation concerns the asymmetry of the lock-in curves about f_n: lock-in occurs more readily for $f_f/f_n > 1$ than it does for $f_f/f_n < 1$. This asymmetry is more pronounced for the flames with coflow (Flames 2 and 5) than for those without coflow (Flames 1, 3, 4, and 6). As we will show in §3.2, simple model equations, such as the VDP oscillator, have symmetric lock-in curves, which means that this asymmetry is a feature of the flow, and not a feature of lock-in. Previous work has shown that when there is competition between two modes at different frequencies, one will take over and saturate nonlinearly before the other [15]. A possible explanation of asymmetric lock-in is that forcing applied at higher frequencies induces higher peak accelerations at the flame base. In isothermal jets, higher peak accelerations have been found to promote vortex-ring formation [16]. Forcing at higher frequencies could therefore cause toroidal vortices to roll up earlier, perhaps closer to the injector. If the vortices caused by the forcing roll up before the vortices caused by the natural global mode, they will dominate, increasing the tendency of the flame to lock in.

The fact that lock-in occurs asymmetrically suggests that there may be other asymmetries between forcing above and below f_n. To investigate this, we show in Fig. 5 contours of the flame response as a function of A and f_f/f_n. As before, the focus is on Flame 5 because it is representative of the globally unstable flames. The flame response, measured at $x/d_1 = 10$, is defined as the ratio of the root-mean-square (RMS) intensity fluctuation with forcing to the same quantity without forcing: $I'_{rms,\,for}/I'_{rms,\,unf}$. Also shown on the figure are selected data from Fig. 4 indicating the onset of lock-in.

As A increases for f_f/f_n slightly above 0.5 or 1 (Fig. 5), the response first decreases below unity, reaches a minimum near the onset of lock-in (circular markers), and then increases back towards unity. For f_f/f_n slightly below 1, however, the response increases above unity and then saturates. Forcing very close to the fundamental causes a response that is between these two extremes. For $f_f/f_n > 1.36$, lock-in is not possible even at high A. Instead, over a wide band of forcing frequencies ($1.36 < f_f/f_n < 2.38$), increasing A causes a gradual rise in the response above unity, which peaks at $A \approx 0.30 - 0.50$ before decreasing for higher A.

In summary, lock-in occurs most readily for flames with weak global instability and when f_f is close to f_n, both of which were expected. It was not expected, however, that the lock-in behaviour would depend on whether f_f is above or below f_n. When forced below f_n, the flame is more resistant to lock-in, but, once it does, its oscillations are stronger than those of the unforced flame. When forced above f_n, the flame is less resistant to lock-in, but, once it does, its oscillations are weaker than those of the unforced flame. The last results suggest that, for thermoacoustic systems, lock-in may not be as detrimental as it is thought to be.

3.2. Modelling

For the VDP oscillator, we consider a case in which the forcing frequency is slightly above the natural frequency: $\omega_f/\omega_n = 1.03$. Time traces of the steady-state solution are shown in Fig. 6a for five forcing amplitudes ($0.05 \le A_{vdp} \le 0.13$) and for the unforced case. The corresponding PSD curves are shown in Fig. 6b. These figures are analogous to those for the flame (Fig. 2).

The forced response of the VDP oscillator is qualitatively similar to that of the flame. When unforced, the VDP oscillator has a dominant natural frequency, represented in the PSD by a sharp peak at $\omega_n = 1$. There are, however, no harmonics because the solution is perfectly sinusoidal.

When forced at a low amplitude ($A_{vdp} = 0.05$), the VDP oscillator responds at ω_f as well as ω_n, with multiple spectral peaks arising between these two frequencies. This suggests that, like the flame, the VDP oscillator is quasiperiodic before lock-in.

As A_{vdp} increases from 0.05 to 0.10, ω_n shifts towards ω_f, which remains fixed. The spectral peaks around ω_n and ω_f become closer and their envelope widens. At $A_{vdp} = 0.112$, that envelope has a subtle bias towards frequencies below ω_n, as evidenced by the more marked tail. Once A_{vdp} reaches a critical value of 0.115, the VDP oscillator locks into the forcing, in much the same way as the flame does.

The similarities between the VDP oscillator and the flame are also apparent in the Poincaré maps (Fig. 6c). When unforced, the solution starts off as a limit cycle, but becomes quasiperiodic as A_{vdp} increases towards lock-in. After lock-in, it converges to a new limit cycle and the phase trajectory converges to a new orbit.

The consolidated PSD (Fig. 7) resembles the analogous plot for the flame (Fig. 3). The vertical stripe is the response of the natural mode. When forced around ω_n, however, that response locks into the forcing, represented by the diagonal stripe. There is no diamond pattern because the VDP oscillator is sinusoidal.

The lock-in map is shown in Fig. 8, with A_{loc} indicated by circular markers. The greyscale is the VDP response, defined as the RMS of the forced solution normalised by that of the unforced solution: $x'_{rms,\,for}/x'_{rms,\,unf}$. This response decreases below unity as A_{vdp} increases towards lock-in, regardless of whether ω_f is above or below ω_n. At lock-in, it reaches a minimum, and its value decreases as ω_f deviates from ω_n. The lock-in curve is $\vee$ shaped and symmetric about ω_n. Although many of these features are observed in the flame, two are not: (i) the flame response at lock-in is above (not below) unity when $f_f < f_n$; and (ii) the flame's lock-in curve is not symmetric about f_n.

4. Conclusions

We have applied acoustic forcing to a range of jet diffusion flames. These flames are hydrodynamically self-excited and thus oscillate at discrete natural frequencies. We applied the forcing around these frequencies, at varying amplitudes, in order to study how they

respond before and after lock-in. We then modelled that response with the forced VDP oscillator.

Contrary to expectations, our results show that a hydrodynamically self-excited flame oscillating at one frequency is not insensitive to forcing at other frequencies. When forced at low amplitudes, it responds at both frequencies, and there is beating, indicating quasiperiodicity.

As the forcing amplitude increases, the flame eventually locks into the forcing. Weakening the global instability – by adding coflow or by diluting the fuel mixture – causes the flame to lock in at lower forcing amplitudes. The critical forcing amplitude required for lock-in increases as the forcing frequency deviates from the natural frequency. This increase is linear, giving rise to a $\vee$-shaped lock-in curve.

The lock-in curve has two subtle asymmetries about the natural frequency. First, a lower forcing amplitude is required for lock-in when the forcing frequency is above the natural frequency. Second, the flame response at lock-in is weaker than the unforced response when the forcing frequency is above the natural frequency, but is stronger than the unforced response when the forcing frequency is below the natural frequency.

Many of these features could be modelled with the forced VDP oscillator. They include (i) the coexistence of the natural and forcing frequencies before lock-in; (ii) the presence of multiple spectral peaks around these competing frequencies, indicating quasiperiodicity; (iii) the occurrence of lock-in above a critical forcing amplitude; (iv) the $\vee$-shaped lock-in curve; and (v) the reduced broadband response at lock-in. There are, however, some features that could not be modelled. They include (i) the asymmetry of the forcing amplitude required for lock-in; and (ii) the asymmetry of the flame response at lock-in.

Our results have conflicting implications for thermoacoustics. On one hand, they show that a flame's response at the forcing frequency cannot be eliminated simply by ensuring that it has a hydrodynamically self-excited mode at another frequency. In fact, the flame responds at several different frequencies, potentially exciting other acoustic modes in the combustor. On the other hand, our results also show that a flame's resistance to lock-in can be enhanced by strengthening its global instability. In industry, this behaviour could be exploited by imparting strong global instability to the flame and ensuring that its oscillation frequency is tuned away from the natural acoustic frequencies of the combustor.

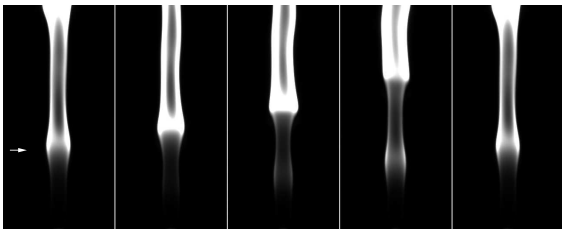

Figure 1: Image sequence of a globally unstable flame (Flame 5) oscillating through one natural cycle. The sequence runs from left to right, and the images are separated in time by a quarter period. The white arrow indicates the axial station at which the data are examined: $x/d_1 = 10$.

References

[1] P. Huerre, P. Monkewitz, Local and global instabilities in spatially developing flows, Annu. Rev. Fluid Mech. 22 (1990) 473–537.

[2] T. Maxworthy, The flickering candle: transition to a global oscillation in a thermal plume, J. Fluid Mech. 390 (1999) 297–323.

[3] M. Juniper, L. Li, J. Nichols, Forcing of self-excited round jet diffusion flames, P. Combust. Inst. 32 (2009) 1191–1198.

[4] K. Sreenivasan, S. Raghu, D. Kyle, Absolute instability in variable density round jets, Exp. Fluids 7 (1989) 309–317.

[5] M. Provansal, C. Mathis, L. Boyer, Bénard-von Kármán instability: transient and forced regimes, J. Fluid Mech. 182 (1987) 1–22.

[6] J. Nichols, P. Schmid, J. Riley, Self-sustained oscillations in variable-density round jets, J. Fluid Mech. 582 (2007) 341–376.

[7] A. Lingens, K. Neemann, J. Meyer, M. Schreiber, Instability of diffusion flames, P. Combust. Inst. 26 (1996) 1053–1061.

[8] D. Durao, J. Whitelaw, Instantaneous velocity and temperature measurements in oscillating diffusion flames, Proc. R. Soc. Lond. A 338 (1974) 479–501.

[9] L. Chen, J. Seaba, W. Roquemore, L. Goss, Buoyant diffusion flames, P. Combust. Inst. 22 (1989) 677–684.

[10] B. van der Pol, J. van der Mark, Frequency demultiplication, Nature 120 (1927) 363–364.

[11] A. Seybert, D. Ross, Experimental determination of acoustic properties using a two-microphone random-excitation technique, J. Acoust. Soc. Am. 61 (1977) 1362–1370.

[12] M. Füri, P. Papas, R. Rais, P. Monkewitz, The effect of flame position on the Kelvin–Helmholtz instability in non-premixed jet flames, P. Combust. Inst. 29 (2002) 1653–1661.

[13] B. Bellows, A. Hreiz, T. Lieuwen, Nonlinear interactions between driven and self-excited acoustic oscillations in a premixed combustor, in: 44th AIAA Aerospace Sciences Meeting, American Institute of Aeronautics and Astronautics, 2006. GT2006-0755.

[14] J. Davitian, D. Getsinger, C. Hendrickson, A. Karagozian, Transition to global instability in transverse-jet shear layers, J. Fluid Mech. 661 (2010) 294–315.

[15] B. Pier, Open-loop control of absolutely unstable domains, P. Roy. Soc. A - Math Phy. 459 (2003) 1105–1115.

[16] C. Külsheimer, H. Büchner, Combustion dynamics of turbulent swirling flames, Combust. Flame 131 (2002) 70–84.

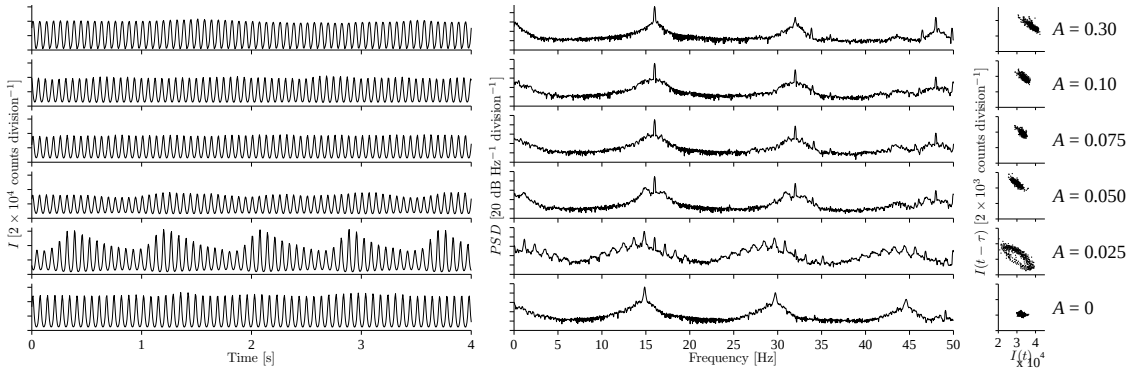

(a) Time trace (b) PSD (c) Poincaré map

Figure 2: (a) Time trace, (b) PSD, and (c) Poincaré map of the intensity from Flame 5 forced at a frequency, $f_f = 16$ Hz, slightly above the natural frequency, $f_n = 14.7$ Hz. The data shown are for five forcing amplitudes, $0.025 \leq A \leq 0.30$, and for the unforced case. The onset of lock-in occurs at $A_{loc} = 0.075$.

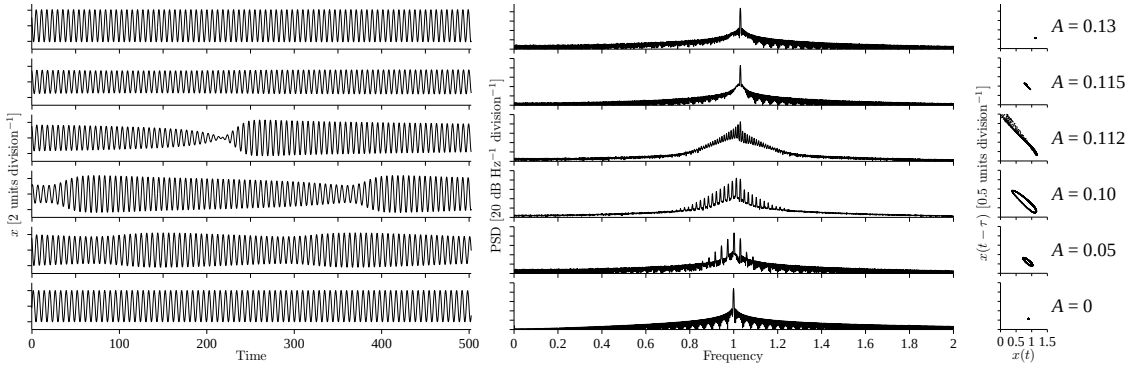

(a) Time trace (b) PSD (c) Poincaré map

Figure 6: (a) Time trace, (b) PSD, and (c) Poincaré map of the VDP oscillator forced at a frequency, $\omega_f = 1.03$, slightly above the natural frequency, $\omega_n = 1$. The solutions shown are for five forcing amplitudes, $0.05 \leq A \leq 0.13$, and for the unforced case. The onset of lock-in occurs at $A_{loc} = 0.115$. This figure can be compared to Fig. 2, which is for a self-excited flame.

Table 1: Flow conditions of the six flames under investigation. GU, globally unstable; GS, globally stable; U_2/U_1, coflow velocity relative to jet velocity; f_n, natural global frequency.

Flame		$[CH_4]$	$[N_2]$	U_2/U_1	f_n [Hz]
1		1.00	0.00	0	12.5
2		1.00	0.00	0.083	13.9
3	GU	0.80	0.20	0	13.0
4		0.60	0.40	0	13.3
5		0.60	0.40	0.083	14.7
6	GS	0.40	0.60	0	14.3[a]

[a]This is for the lightly damped global mode, which arises only with forcing. When unforced, Flame 6 is globally stable, with two weak modes at 14.8 and 16.1 Hz.

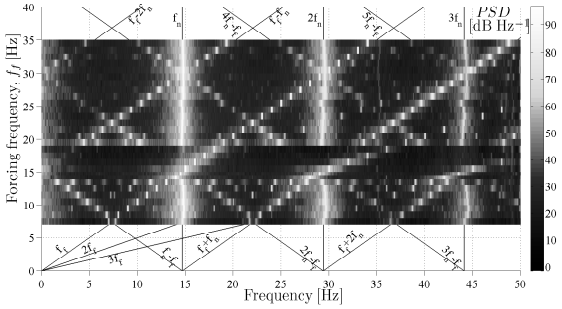

Figure 3: Consolidated PSD for Flame 5 forced at $A = 0.10$.

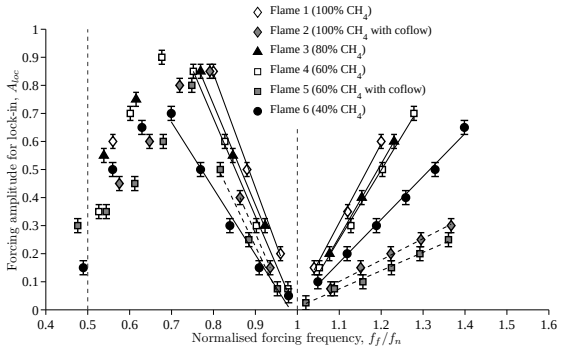

Figure 4: Lock-in map for CH_4–N_2 jet diffusion flames. The diagonal lines through the data around $f_f/f_n = 1$ are linear fits. The error bars denote the increment by which the forcing amplitude is varied.

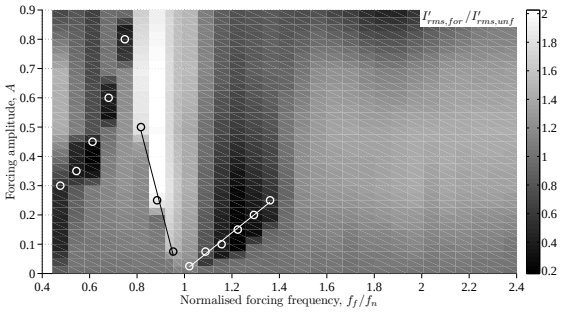

Figure 5: Response of Flame 5 as a function of forcing amplitude and frequency. The circular markers denote the onset of lock-in.

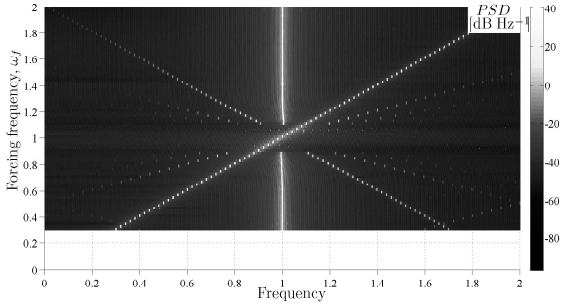

Figure 7: Consolidated PSD for VDP oscillator forced at $A_{vdp} = 0.30$. This figure can be compared to Fig. 3, which is for a self-excited flame.

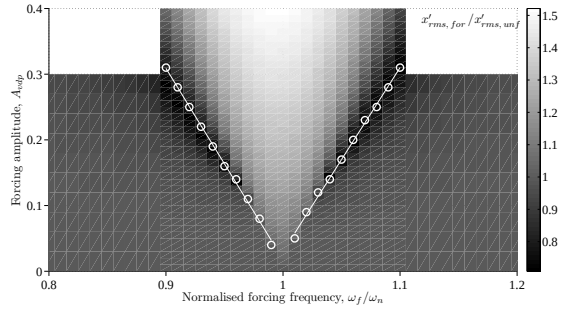

Figure 8: Response of VDP oscillator as a function of forcing amplitude and frequency. The circular markers denote the onset of lock-in. This figure can be compared to Fig. 5, which is for a self-excited flame.